A MATHEMATICAL MODEL FOR THE ENHANCED CYTOPLASMIC TRANSPORT
How to Get (Faster) to the Nucleus

Luna Dimitrio
Dipartimento Me.Mo.Mat., Università degli Studi "La Sapienza" di Roma, Rome, Italy
INRIA Rocquencourt, Domaine de Voluceau, Rocquencourt, France

Roberto Natalini
Istituto per le Applicazioni del Calcolo "M. Picone", Consiglio Nazionale delle Ricerche, Rome, Italy

Luciano Milanesi
Istituto di Tecnologie Biomediche, Consiglio Nazionale delle Ricerche, Segrate, Milano, Italy

Keywords: Cytoplasmic enhanced transport, Microtubules, Partial differential models.

Abstract: We consider a simple model for signal transport in the cytoplasm. Following some recent experimental evidences, the standard diffusion model is supplemented by advection operated through an attachement/detachement mechanism along microtubules. This model is given by a system of partial differential equations which are cast in different dimensions and connected by suitable exchange rules. A numerical scheme is introduced and some simulations are presented and discussed to show the performances of our model.

1 INTRODUCTION

A key process in cell's life is intra-cellular transport. Eukaryotes have a highly compartmentalized structure: different processes are performed in specific compartment named organelles. The largest organelle is of course the nucleus, where DNA is stored and protected. Proteins need to get into the nucleus to activate specific processes and to exchange information. There are different mechanisms that the cell can exploit to this purpose. For example proteins can move from a region of higher concentration to one of lower concentration: this process is known as facilitated transport. The concentration gradient that allows this kind of transport is created by the protein Ran that in its GDP and GTP bound form operates in import and export of proteins from and to the nucleus. Ran has an asymmetric distribution within the cell: the GTP bound form is abundant in the nucleus while the cytoplasm is rich of Ran•GDP. The Ran gradient operates in the transport mechanism giving the directionality to transport. Other possibilities for nuclear proteins import have been explored and different mechanisms have been proved to cooperate in transport (for a review see (Wagstaff and Jans, 2009)). For example some specific proteins like p53, p38 or the parathyroid hormone-related protein (PTHrP) use microtubules to facilitate their way towards the nucleus (Giannakakou et al., 2002; Roth et al., 2007; Lam et al., 2002; Gong et al., 2010).

We are interested in this kind of transport where proteins use microtubules as further support through their way to the nucleus. In this work we would like to point out the importance of microtubule-assisted transport for an efficient nuclear accumulation of NLS-proteins. To further motivate this work let us remark that objections were raised against the theory that diffusion alone is the only mechanism operating in transport (Agutter et al., 1995). For example cytoplasmic location of enzymes in signaling cascades (Kholodenko, 2009) is fundamental for the efficient diffusion of the signal within the cell.

We present here a spatial model based on PDEs whose variables are the proteins concentrations and

Dimitrio L., Natalini R. and Milanesi L..
A MATHEMATICAL MODEL FOR THE ENHANCED CYTOPLASMIC TRANSPORT - How to Get (Faster) to the Nucleus.
DOI: 10.5220/0003135700390046
In *Proceedings of the International Conference on Bioinformatics Models, Methods and Algorithms* (BIOINFORMATICS-2011), pages 39-46
ISBN: 978-989-8425-36-2

we restrict our study to an area assumed to be influenced by a single microtubule. We want to represent two different transport mechanisms: diffusion and active transport along microtubules. Since we are interested in transport of nuclear protein, we will look at transport along microtubules in a single direction, i.e. towards the nucleus.

For a matter of simplicity we chose to describe only the essential molecular pathways and we get a simple model with two species concentrations and the concentration of the attached particles, represented by a third equation.

Moreover as a distinguishing feature we model the transported cargo concentration on the microtubule by a 1-dimensional process, and we let the diffusive molecules lie on the two dimensional domain. This multidimensional approach is largely used in blood-flow numerical modeling in order to describe large systems of vessels: they give the possibility to switch from 3D models to 1D or 0D representations and recreate dynamics that involve different space scales in large vessels networks. This choice consents also a gain in computational time, see for instance (Passerini et al., 2009).

1.1 Microtubules Enhanced Transport

Microtubules (MTs) are filaments composed by tubulin dimers that constitute the cytoskeleton together with actin filaments and intermediate filaments. They are organized in a radial structure pointing towards a common region, the Microtubule Organizing Center (MTOC), from which they nucleate. The MTOC is set near the nucleus so that microtubules irradiate from the cell center to the cell periphery. Moreover they have a polarity: a plus end toward the cell periphery and a minus at the cell center.

Microtubules are involved in many cellular process, namely they are responsible for vesicles and organelles transport within the cell, they play an important role during mitosis and are required in cellular motility. Here, we are interested in investigating the ability of microtubules to enhance intracellular transport. It is known that viruses use these highways to get close to the nucleus (Campbell and Hope, 2003) and that vesicles and organelles, as mitochondria, are transported within the cytoplasm by motor proteins bound to microtubules.

As said before recent studies demonstrated that some proteins use this network to facilitate their way towards the perinuclear region (Giannakakou et al., 2002; Roth et al., 2007; Lam et al., 2002; Gong et al., 2010; Salman et al., 2005). Regulation of the cellular machinery need an efficient transport machinery and the cytoskeleton that structure the entire cytoplasm seems to be a natural candidate to cover this role (Wagstaff and Jans, 2009; Campbell and Hope, 2003). In order to move close to the nuclear envelope, viruses, organelles and some NLS-proteins take advantage of the microtubule network. In some cases molecules can associate to this structure to prevent their nuclear accumulation (Campbell and Hope, 2003). Active transport along the MTs is permitted by binding to a *motor* protein, which possesses a mechanism for moving along the MT at a speed of about 0.5 to $1\,\mu m\,s^{-1}$ (Smith and Simmons, 2001; Nédélec et al., 2001). Two families of motor proteins associate to the MTs: dynein, which permits transport from the plus end to the minus end, and kinesin, which transports in the opposite direction. Here we just focus our model on the dynein motor.

2 A SIMPLE MODEL

A few mathematical models exist to represent these different employs of MTs (Cangiani and Natalini, 2010; Smith and Simmons, 2001; Dinh et al., 2007) but most of them are one dimensional models and do not consider the effective position of single filaments. Recently Cangiani and Natalini proposed in (Cangiani and Natalini, 2010) a three dimensional model of nucleocytoplasmic transport which takes into account all the signalling pathway of protein import. Their results show the dependence on MT-enhanced transport for the optimality of nuclear import, as reported in Roth (Roth et al., 2007).

In this paper we propose a model that could reproduce microtubule-based transport towards the nucleus to highlight the importance of this mechanism for the efficiency of nuclear import. To this goal we suggest a simplified bi-dimensional model of cytoplasmic transport taking into account as few kinetic processes as possible.

Unlike other models we represent the position of a single MT filament. For the time being we do not want to model the crossing of the nuclear envelope and we restrict our study to the representation of a single domain that called Ω (see Figure 1). Furthermore we will consider only the kinetics of the free cargo and of the cargo-dynein complex without looking at the whole import pathway. We model this system so that transported particles obey to a one dimensional equation, while diffusing particles are in a two dimensional domain. We restrict our study to an area that we suppose influenced by a single microtubule. Finally, via the choice of periodic boundary condition on the longer side of our domain, we make the

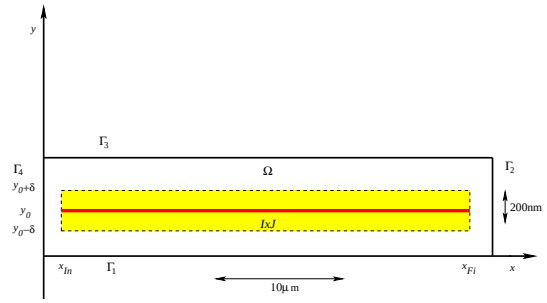

Figure 1: Area of the cytoplasm where intracellular transport is modeled: $\Omega = [0, L_x] \times [0, L_y]$. The yellow rectangle ($I \times J = [x_{In}, x_{Fi}] \times [y_0 - \delta, y_0 + \delta]$) represents the attraction area of the microtubule filament, the red strip is the microtubule, positioned in y_0.

assumption that MTs are homogeneously distributed inside the cell.

2.1 A Model for Proteins

We consider only the kinetic equations of two proteins: a generic NLS-protein (cargo C) that has to be transported to the nucleus and the motor protein dynein (D). Dynein is a molecular motor that move along microtubules in the direction of cell nucleus (Mallik et al., 2005). We suppose dynein concentration constant and uniformly distributed. Cargo diffuses freely in the cytosol and bind to dynein, so that facilitated diffusion can be achieved. If the dynein-cargo complex (P_f) reach the attraction area (see Figure 1) of the microtubule filament, they can bind together, so attachment and detachment to the MT is seen as a kinetic process.

Once the complex (P_t) moves on the microtubule, it has a steady velocity of about $1 \mu m s^{-1}$ as reported, for example, in (Nan et al., 2005). The complex bound to the MT has a certain probability k_{-1} to detach from the filament. However at the end of the microtubule it is necessarily released near the boundary of the considered region. Here we specify the kinetic reactions:

$$D + C \underset{k_-}{\overset{k}{\rightleftharpoons}} P_f,$$

$$P_f \underset{k_{-1}}{\overset{k_1}{\rightleftharpoons}} P_t \qquad \text{on } I\text{x}J.$$

The last reaction occurs only in the area of attraction of the microtubule, here denoted as IxJ (see Figure 1). Here $I = [x_{In}, x_{Fi}]$ is the actual length of the microtubule and $J = [y_0 - \delta, y_0 + \delta]$ is the width of the filament positioned in y_0.

2.2 The Mathematical Model

We want to represent mathematically the molecular pathways presented above, localizing them in the considered domain Ω : in this way we get a system of partial differential equations. We imagine the domain to be the cytoplasmic area surrounding a single filament of microtubule. We assume that the structure of the MTs network is homogeneous within the cell and represent this choice via periodic boundary condition on the long sides of the domain, Γ_1 and Γ_3.

We use classic laws to represent every process: Mass Action Law for kinetic reactions, Fick's law of free diffusion for species concentrations diffusion and active transport for the particle bound to the microtubule. Let $u = [C]$, $v = [P_f]$, $w = [P_t]$ be respectively the cargo, cargo+dynein and transported complex concentrations, d_u and d_v the diffusion coefficients of the u and v species respectively and c the

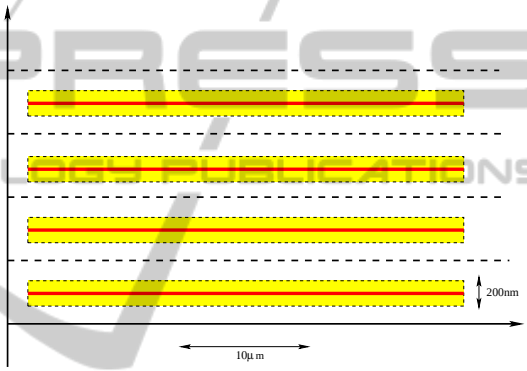

Figure 2: Periodic boundary conditions on the long side of the domain (see figure 1) in equation 1 make the cell an homogenous environment. This means that the strip where we model the system is only a "zoom" on a single microtubule. We suppose that the same reactions take place in the rest of the cell.

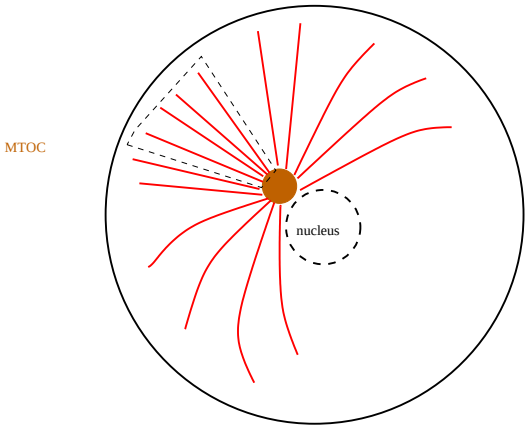

Figure 3: Schematic model of the cell with its microtubules structure.

$$\begin{cases} \dfrac{\partial u}{\partial t} = d_u \Delta u - k d_{dyn} u + k_{-} v, & \text{in } \Omega, \\ \dfrac{\partial v}{\partial t} = d_v \Delta v + k d_{dyn} u - k_{-} v - k_1 v \mathbb{1}_{\mathbf{IxJ}} + k_{-1} w \frac{\mathbb{1}_{\mathbf{IxJ}}}{|J|} + c(\delta_{x_{Fi}} - \delta_{x_{In}}) w \frac{\mathbb{1}_{\mathbf{IxJ}}}{|J|}, & \text{in } \Omega, \\ \dfrac{\partial w}{\partial t} + c \dfrac{\partial w}{\partial x} = -k_{-1} w + k_1 \int_J v dy, & \text{in }]x_{In}, x_{Fi}[, \end{cases} \tag{1}$$

motor velocity for the transported particle. Dynein concentration is supposed to be constant and is denoted by $[D] = d_{dyn}$.

Under the previous assumptions the u and v species satisfy a reaction-diffusion equation, while w is controlled by a convection equation modeling the transport along the microtubule with a steady velocity c. The model we get is equation 1, where δ_{x_0} in the equation for v stands for the Dirac mass in $x_0 = x_{In}, x_{Fi}$. The term $c(\delta_{x_{Fi}} - \delta_{x_{In}}) w \mathbb{1}_{\mathbf{IxJ}}$ represents the contribution due to the outgoing flux of the transported particles at the end of the MT filament and it guarantees conservation of the mass. We also impose the boundary conditions:

$$\begin{cases} \dfrac{\partial u}{\partial n} = 0, \ \dfrac{\partial v}{\partial n} = 0, & \text{on } \Gamma_4, \\ d_u \dfrac{\partial u}{\partial n} + p_u u = 0, \ d_v \dfrac{\partial v}{\partial n} + p_v v = 0, & \text{on } \Gamma_2, \\ w(x_{In}) = 0. \end{cases}$$

As said before, the boundary conditions on Γ_1 and Γ_3 for u and v are periodic, i.e. we suppose that for every t $u|_{\Gamma_1} = u|_{\Gamma_3}$, respectively v (see figure 2). We assume that proteins cannot cross the membrane layer on Γ_4 using a Neumann homogeneous boundary condition, but we suppose that on Γ_2 there is an outgoing flow proportional to the species concentration. For the transported cargo we suppose that there is not an upcoming flux at the beginning of the microtubule.

We remark that the two first equations lie in a two dimensional domain: $u = u(x,y,t)$ and $v = v(x,y,t)$ represent the species concentration per unit volume at time t in $(x,y) \in \Omega$. The equation for w is one dimensional and the cargo concentration can move only in one direction along the filament, positioned at $[x_{In}, x_{Fi}] \times \{y_0\} \subset \Omega$.

In our model, to point out the difference in the type of transport mechanisms, we consider the MT dependent transport to be 1D and describe diffusion as a bidimensional event. With this approach we couple the two mechanisms considered and model them at two different levels. In this way we get an interconnected system that relies on the two processes but emphasizes the features of each type of transport.

A concentration gradient that allows diffusion in the whole domain, and active transport directed towards the nucleus and localized near the microtubule.

3 SCHEME

In this section we will propose a numerical scheme in order to solve the system presented above.

Let us introduce a space discretization of the x and y axis. Our domain Ω is the rectangle $[0, L_x] \times [0, L_y]$ (fig: 1). We denote by Δx, Δy the discretization steps in the x and y directions respectively and we divide the intervals $[0, L_x]$ and $[0, L_y]$ in $N_x + 1$ and $N_y + 1$ points. The mesh points will be $(x_i, y_j) = (i\Delta x, j\Delta y)$ with $0 \le i \le N_x + 1$, $0 \le j \le N_y + 1$. Let Δt be the time discretization step and t_n the n^{th} step, i.e. $t_n = n\Delta t$, $n \in \mathbb{N}$. According to these notations $u^n_{i,j}$ will be the approximation of the solution of u in (x_i, y_j) at time t^n and respectively $v^n_{i,j}$ and w^n_i denote the approximations of v and w. We remark that w lies in $[x_{In}, x_{Fi}]$ so w^n_i is well defined only for certain values of i, in particular we need $x_{In}/\Delta x \le i \le x_{Fi}/\Delta x$.

We first solve the third equation of the system. We discretize the transport contribution by using an upwind scheme enhanced by a TDV flux limiter (Sweby, 1984). The right hand side is made by two parts. The term $-k_{-1} w$ is stiff, and it will be approximated by an implicit discretization. For the other source term $F := \frac{\int_J v(x_i, y) dy}{|J|}$, we used an upwinding scheme (Roe, 1981), which improve the resolution near the asymptotic states, and besides, we approximated the integral using a trapezoidal rule. Summing up these considerations, we obtain a scheme for w (equation 2). In this equation $\nu = c\frac{\Delta t}{\Delta x}$ and we put $r_{i+1/2} = \frac{w^n_{i-1} - w^n_{i-2}}{w^n_i - w^n_{i-1}}$ and $r_{i-1/2} = \frac{w^n_{i+1} - w^n_i}{w^n_i - w^n_{i-1}}$, while ϕ is a flux limiter function (minmod in our simulations, see again (Sweeby, 1984)).

We use a IMEX midpoint scheme (Briani et al., 2007), to solve numerically the reaction-diffusion system (see equations: 3, 4), where

$$\frac{\delta_x^2 u^{(1)}}{\Delta x^2} = \frac{u^{(1)}_{i+1,j} - 2u^{(1)}_{i,j} + u^{(1)}_{i-1,j}}{\Delta x^2}$$

and

$$\begin{aligned}(1+\Delta t k_{-1})w_i^{n+1} \quad &= w_i^n - \tfrac{\nu}{2}(w_{i+1}^n - w_{i-1}^n) - \tfrac{\nu}{2}(1-\nu)[\phi(r_{i+1/2})(w_{i+1}^n - w_i^n) \\ &+\phi(r_{i-1/2})(w_i^n - w_{i-1}^n)] + \tfrac{1}{2}\Delta t k_1 (F_i^n + F_{i-1}^n).\end{aligned} \tag{2}$$

$$\begin{cases} u_{i,j}^{(1)} = u_{i,j}^n + d_u \frac{\Delta t}{2}(\frac{\delta_x^2 u^{(1)}}{\Delta x^2} + \frac{\delta_y^2 u^{(1)}}{\Delta y^2}) - k d_{dyn}\frac{\Delta t}{2} u_{i,j}^{(1)} + k_- \frac{\Delta t}{2} v_{i,j}^n, \\ v_{i,j}^{(1)} = v_{i,j}^n + d_v \frac{\Delta t}{2}(\frac{\delta_x^2 v^{(1)}}{\Delta x^2} + \frac{\delta_y^2 v^{(1)}}{\Delta y^2}) - k_- \frac{\Delta t}{2} v_{i,j}^{(1)} + k d_{dyn}\frac{\Delta t}{2} u_{i,j}^n, \end{cases} \tag{3}$$

$$\begin{cases} u_{i,j}^{n+1} = u_{i,j}^n + d_u \Delta t(\frac{\delta_x^2 u^{(1)}}{\Delta x^2} + \frac{\delta_y^2 u^{(1)}}{\Delta y^2}) - k d_{dyn}\Delta t u_{i,j}^{(1)} + k_- \Delta t v_{i,j}^{(1)}, \\ v_{i,j}^{n+1} = \begin{cases} v_{i,j}^n + d_v \Delta t(\frac{\delta_x^2 v^{(1)}}{\Delta x^2} + \frac{\delta_y^2 v^{(1)}}{\Delta y^2}) - k_- \Delta t v_{i,j}^{(1)} + k d_{dyn}\Delta t u_{i,j}^{(1)} \\ \quad -k_1 v_{i,j}^n + k_{-1}\frac{w_i^{n+1}}{|J|} & \text{if } i,j \in I \times J\,, \\ v_{i,j}^n + \Delta t(\frac{\delta_x^2 v^{(1)}}{\Delta x^2} + \frac{\delta_y^2 v^{(1)}}{\Delta y^2}) - k_- \Delta t v_{i,j}^{(1)} + k d_{dyn}\Delta t u_{i,j}^{(1)} - k_1 v_{i,j}^n \\ \quad +k_{-1}\frac{w_i^{n+1}}{|J|} + c w_i^{n+1} & \text{if } (i,j)|(x_i,y_j) = (x_{Fi},y_0) \\ v_{i,j}^n + d_v \Delta t(\frac{\delta_x^2 v^{(1)}}{\Delta x^2} + \frac{\delta_y^2 v^{(1)}}{\Delta y^2}) - k_- \Delta t v_{i,j}^{(1)} + k d_{dyn}\Delta t u_{i,j}^{(1)} & \text{otherwise.} \end{cases} \end{cases} \tag{4}$$

$$\frac{\delta_y^2 u^{(1)}}{\Delta y^2} = \frac{u_{i,j+1}^{(1)} - 2u_{i,j}^{(1)} + u_{i,j-1}^{(1)}}{\Delta y^2}$$

(respectively for v). since u and v satisfy mixed boundary conditions on Γ_2 and Neumann boundary conditions on Γ_4 we use the second order derivative approximation to calculate the boundary values. We use this second order approximation

$$\frac{\partial u}{\partial n}(0,y_j) = \frac{1}{2\Delta x}(-3u_{0,j}^n + 4u_{1,j}^n - u_{2,j}^n),$$

to yield:

$$u_{0,j}^n = (\frac{4}{3}u_{1,j}^n - \frac{1}{3}u_{2,j}^n).$$

We also discretize:

$$\frac{\partial u}{\partial n}(L_x,y_j) = \frac{1}{2\Delta x}(3u_{N_x+1,j}^n - 4u_{N_x,j}^n + u_{N_x-1,j}^n),$$

which gives

$$u_{N_x+1,j}^n = \frac{d_u}{d_u + 2\Delta x p_u}(4u_{N_x,j}^n - u_{N_x-1,j}^n).$$

Similarly we calculate the numerical approximation of v on the boundary.

3.1 Numerical Experiments

In this section we will do some numerical experiments and we will analyze the order of accuracy of the scheme proposed. We will solve the system and evaluate the differences of solutions at the final time T=2. To do this we will change the space step and calculate the L^1 norm of the difference between numerical solutions at different space steps. We put $h = \Delta x = \Delta y$ and define the function

whose values represent the order of accuracy of the numerical solution. The time step Δt will change accordingly to h to satisfy the CFL condition for the advection equation and the condition for IMEX midpoint scheme stability, so that in each experiment we get $\Delta t = min(h/c, h^{4/3})$, see (Briani et al., 2007) for more details.

We fix all the reactions constants and of course the diffusion constants of the two species:

$$k = 0.2, \quad k_- = 0.2, \quad k_1 = 5, \quad k_{-1} = 0.2, \quad d_u = 10,$$
$$d_v = 8, \quad c = 1.$$

We fixed the motor velocity $c = 1$, as found in literature (Mallik et al., 2005), as well as the attachment and detachment rate of cargo and dynein (see (Cangiani and Natalini, 2010)). The total dynein concentration is constant and we assume [D]=1. The diffusion constants are relative to a given cargo protein. For example p53-GFP diffusion constant was estimated to be $15.4\mu m^2 s^{-1}$. Table 1 shows the L^1 distances of solutions at different space steps. Table 2 shows the numerical accuracy of the scheme.

4 RESULTS

Using the scheme presented in the previous section, we solve numerically the reaction-diffusion-advection system to calculate the net flux of particles with and without microtubules. Our purpose is to show that microtubule activity is a natural support for intracellular trafficking.

Many proteins have been proved to use the MTs

Table 1: Distance calculated in L^1 for solutions at different space steps.

h	$\|u^n(h)-u^n(h/2)\|_1$	$\|v^n(h)-v^n(h/2)\|_1$	$\|w^n(h)-w^n(h/2)\|_1$
0.02	$2.8810\cdot10^{-4}$	0.0013	0.0352
0.01	$8.8866\cdot10^{-5}$	$3.8236\cdot10^{-4}$	0.0393
0.005	$4.3167\cdot10^{-5}$	$2.0382\cdot10^{-5}$	0.0412
0.0025	$1.9924\cdot10^{-5}$	$1.0474\cdot10^{-4}$	$1.0611\cdot10^{-4}$

Table 2: Numerical order of accuracy, defined by $\gamma_f = \log_2 \frac{\|f^n(h)-f^n(h/2)\|_1}{\|f^n(h/2)-f^n(h/4)\|_1}$.

h	γ_u	γ_v	γ_w
0.02	1.6968	1.7677	0.8399
0.01	1.0418	0.9079	0.9323
0.005	1.1157	0.9611	0.9638

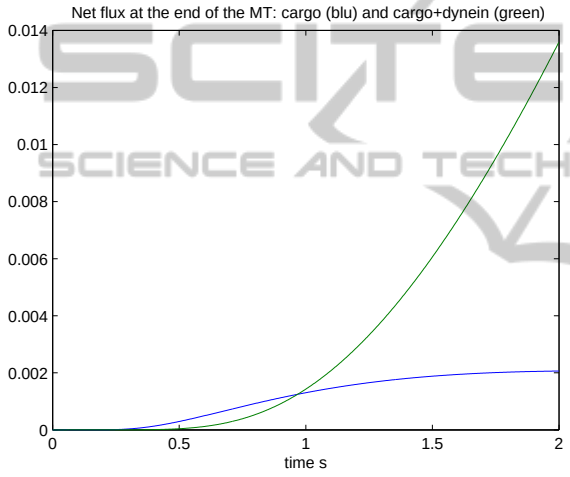

Figure 4: Net flux is calculated at the end of the MT filament: CARGO (blue) and CARGO+DYNEIN (green).

network and the motor protein dynein to facilitate their way towards the nucleus. Maybe the most notable is the tumor proteins p53, because of its crucial role in cell life regulation (Roth et al., 2007; Giannakakou et al., 2002). But other proteins, as p38 or PTHrP are known to be transported by motor proteins to improve nuclear accumulation (Gong et al., 2010; Lam et al., 2002).

We performed different numerical experiments to simulate the presence or not of the microtubule in our domain. In in vitro experiments ((Roth et al., 2007)), microtubules dynamics is suppressed by the use of specific drugs. In this way cargo can not be transported along the filament. We can easily simulate these two different states of the cell uncoupling the third equation of the system.

Our results reproduce qualitatively the behaviour reported in experiments the by Roth *et al*. We calculated the net flux of each species at the end of the

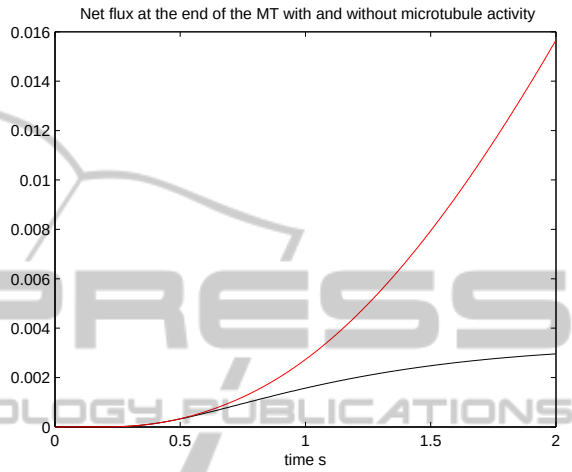

Figure 5: The net flux without MT (black) and with MT (red). As expected, simulations show that the MTs activity facilitate transport mechanism and makes it more efficient.

microtubule. This is to say we calculated $\phi_u(t) = -d_u \int_0^{L_y} \nabla u \cdot \mathbf{n} dy$ and $\phi_v(t) = -d_v \int_0^{L_y} \nabla v \cdot \mathbf{n} dy$. As we can see in figure 5 the net flux is higher if the microtubule structure is used for protein trafficking. In the same way we remark that the flux of the v species is greater then the flux of the diffusive species u.

In figure 6 we can see the different profiles of u and v at the final time T. In the case of simple diffusion a natural homogenization process just began. When microtubule is activated we can see a great difference in the total concentration profile and remark the relevance of active transport.

5 CONCLUSIONS

With this simple model we aimed to reproduce a mechanical behaviour of signal transport in the cytoplasm and to highlight the importance of microtubule activity. It is still unknown why some proteins use MTs unlike others. We found a clear difference in the results (total net flux enhanced thanks to microtubule based transport) for cargoes that do use this mechanics to move faster towards the nucleus. Our purpose was not to reproduce data found in literature but to point out the importance of this second mechanism

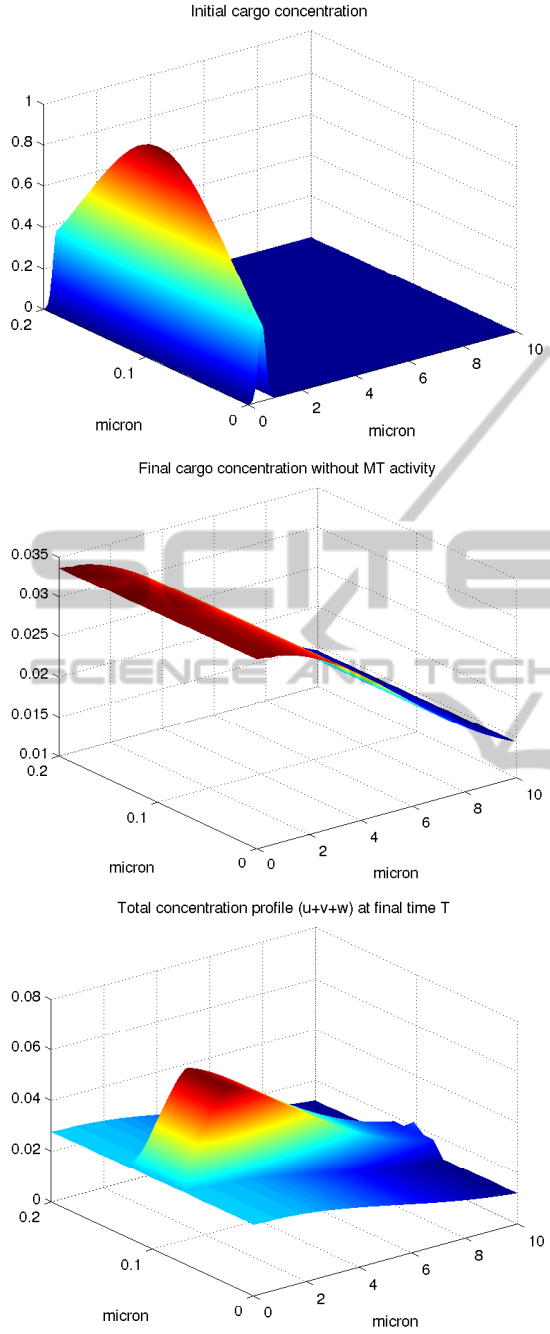

Figure 6: Top: Initial cargo concentration. Middle: final cargo concentration at T=2, without microtubule support. Bottom: total concentration profile at T=2 with microtubule activity.

that has recently been explored as a nuclear protein trafficking support. Furthermore proteins like p53 or PTHrP that are tumor suppressors and regulate cell life have been proved to use the MT network and this motivate further our study.

Using a PDEs system of equation, with a spatial representation of the concentration cargo, we could compare the diffusion mechanism against the advection one. Our multidimensional approach was a tool to stress the difference in the two types of transport, which will be compared in the future to more data in the literature.

ACKNOWLEDGEMENTS

This work has been supported by CNR Italian Bioinformatics Network, MIUR FIRB (RBPR05ZK2Z) (RBPIN064YAT_003).

REFERENCES

Agutter, P. S., Malone, P. C., and Wheatley, D. N. (1995). Intracellular transport mechanisms: a critique of diffusion theory. *J Theor Biol*, 176(2):261–272.

Briani, M., Natalini, R., and Russo, G. (2007). Implicit-explicit numerical schemes for jump-diffusion processes. *Calcolo*, 44:33–57.

Campbell, E. M. and Hope, T. J. (2003). Role of the cytoskeleton in nuclear import. *Adv Drug Deliv Rev*, 55(6):761–771.

Cangiani, A. and Natalini, R. (2010). A spatial model of cellular molecular trafficking including active transport along microtubules. *J Theor Biol*.

Dinh, A.-T., Theofanous, T., and Mitragotri, S. (2007). Modeling of pattern regulation in melanophores. *J Theor Biol*, 244(1):141–153.

Giannakakou, P., Nakano, M., Nicolaou, K. C., O'Brate, A., Yu, J., Blagosklonny, M. V., Greber, U. F., and Fojo, T. (2002). Enhanced microtubule-dependent trafficking and p53 nuclear accumulation by suppression of microtubule dynamics. *Proc Natl Acad Sci U S A*, 99(16):10855–10860.

Gong, X., Ming, X., Deng, P., and Jiang, Y. (2010). Mechanisms regulating the nuclear translocation of p38 map kinase. *J Cell Biochem*.

Kholodenko, B. N. (2009). Spatially distributed cell signalling. *FEBS Lett*, 583(24):4006–4012.

Lam, M. H. C., Thomas, R. J., Loveland, K. L., Schilders, S., Gu, M., Martin, T. J., Gillespie, M. T., and Jans, D. A. (2002). Nuclear transport of parathyroid hormone (pth)-related protein is dependent on microtubules. *Mol Endocrinol*, 16(2):390–401.

Mallik, R., Petrov, D., Lex, S. A., King, S. J., and Gross, S. P. (2005). Building complexity: an in vitro study of cytoplasmic dynein with in vivo implications. *Curr Biol*, 15(23):2075–2085.

Nan, X., Sims, P. A., Chen, P., and Xie, X. S. (2005). Observation of individual microtubule motor steps in living cells with endocytosed quantum dots. *J Phys Chem B*, 109(51):24220–24224.

Nédélec, F., Surrey, T., and Maggs, A. C. (2001). Dynamic concentration of motors in microtubule arrays. *Phys. Rev. Lett.*, 86(14):3192–3195.

Passerini, T., Luca, M. D., Formaggia, L., Quarteroni, A., and Veneziani, A. (2009). A 3d/1d geometrical multiscale model of cerebral vasculature. *Journal of Engineering Mathematics*, 64:319–330.

Roe, P. (1981). Approximate riemann solver, parameter vectors, and difference schemes. *J. Comp. Phys.*, 43:357–372.

Roth, D. M., Moseley, G. W., Glover, D., Pouton, C. W., and Jans, D. A. (2007). A microtubule-facilitated nuclear import pathway for cancer regulatory proteins. *Traffic*, 8(6):673–686.

Salman, H., Abu-Arish, A., Oliel, S., Loyter, A., Klafter, J., Granek, R., and Elbaum, M. (2005). Nuclear localization signal peptides induce molecular delivery along microtubules. *Biophys J*, 89(3):2134–2145.

Smith, D. A. and Simmons, R. M. (2001). Models of motor-assisted transport of intracellular particles. *Biophys J*, 80(1):45–68.

Sweby, P. K. (1984). High resolution schemes using flux limiters for hyperbolic conservation laws. *SIAM J. Numer. Anal.*, 21(5):995–1011.

Sweeby, P. (1984). High resolution schemes using flux-limiters for hyperbolic conservation laws. *SIAM J. Num. Anal.*, 21:995–1011.

Wagstaff, K. M. and Jans, D. A. (2009). Importins and beyond: non-conventional nuclear transport mechanisms. *Traffic*, 10(9):1188–1198.